Narrow-Band Red Emitting Oxonitridosilicate Phosphor $La_{4-x}Sr_{2+x}Si_5N_{12-x}O_x$: Pr^{3+} (x≈1.69)

Hong-Wei Zheng, [a] Xiao-Ming Wang, *[a] Heng-Wei Wei, [a] Yu Zheng, [a] Cong-Ling Yin, [b] Zu-Pei Yang, [c] and Huan Jiao *[a]

Electronic Supplementary Information (ESI):

Materials and synthesis.

The raw materials LnN (Ln = La, Ce; 99%, Yantai Xierde), Sr_3N_2 (99.5%, Hebei LiFu), and α-Si_3N_4 (99.5%, Alfa Aesar) were adequately mixed and ground in an agate mortar. The mixtures were filled into a tungsten crucible. All the above steps were carried out in an Argon-filled glovebox (H_2O < 1 ppm, O_2 < 1 ppm). Subsequently, the tungsten crucible was placed in a gas pressure sintering furnace (ChenHua, ZTQ-45-20) under 1.0 MPa N_2 (90%): H_2 (10%) atmosphere, heated from ambient temperature to 1500℃ within 2 h, maintained at 1500℃ for 8h, cooled down 1200℃ for 6h, and finally quenched to room temperature. The reaction yields yellow crystals for Ln = La and dark gray crystals for Ln = Ce. The rare-earth doped $La_{2.31}Sr_{3.69}Si_5N_{10.31}O_{1.69}$ were made similarly by the addition of EuN (99%, Yantai Xierde), PrF_3 (AR, HWRK Chem), CeN (99%, Yantai Xierde), or $TbCl_3$ (AR, HWRK Chem) to the raw materials while yielded earthy, yellow, light brown, or yellow powders, respectively. Rare-earth doped compounds show no luminescence under irradiation with UV light except Pr^{3+}-doped sample with red emission.

Characterization

Single Crystal X-ray Diffraction. The single crystal of $La_{2.31}Sr_{3.69}Si_5N_{10.31}O_{1.69}$ was picked in the powder samples under an optical microscope using a 50 μm mounted CryoLoop (Hampton). There is no special crystal growth operation for this compound. The Single-crystal X-ray diffraction (XRD) data was collected on Rigaku diffraction (XtaLAB Synergy-R) with a microfocus rotating anode X-ray source diffractometer. An empirical absorption correction using spherical harmonics, implemented in SCALE3 ABSPACK scaling algorithm, was executed to the intensity datasets. The crystal structure of $La_{2.31}Sr_{3.69}Si_5N_{10.31}O_{1.69}$ was solved by SHELXT and refined by SHELXL utilizing Olex2 as a graphical interface. Further details on the crystal structure investigation can be obtained from the Cambridge Crystallographic Data Centre (CCDC) on quoting the depository number CCDC code 2062994, 2063106.

Powder X-ray Diffraction. X-ray diffraction (XRD) data were collected using a Rigaku MiniFlex600 (Japan) diffractometer (Cu Kα radiation, D/teX Ultra high-speed 1D detector). Data collections were carried out over a 2ϑ range from 5° to 120° in a step-mode with 0.01°. Rietveld refinement for $Ln_{4-x}Sr_{2+x}Si_5N_{12-x}O_x$ (Ln = La, Ce) both were performed with TOPAS 5 software.

EDX Spectroscopy. The morphology of the crystalline sample for $Ln_{4-x}Sr_{2+x}Si_5N_{12-x}O_x$ (Ln = La, Ce) powder was investigated by scanning electron microscopy (SEM, Philips-FEI Quanta 25, America) at an accelerating voltage of 5 kV. The chemical composition was confirmed by an attached energy-dispersive X-ray spectrometer (Bruker EDX-XFlash6/30 detector) at an accelerating voltage of 15 kV.

UV/vis Spectroscopy. The diffuse reflection spectrum was measured on a Lambd 1050 UV-vis-NIR spectrophotometer (Perkin-Elmer) in the range from 200 nm to 1200 nm with 1 nm per step size, while the white powder $BaSO_4$ was used as a reference standard.

Density Functional Theory. The band structure and density of states (DOS) of $Ln_{4-x}Sr_{2+x}Si_5N_{12-x}O_x$ (Ln = La, Ce) calculations were performed using density functional theory (DFT) and the Cambridge Serial Total Energy Package (CASTEP) code, where the spin-polarized magnetic is included. The plane-wave basis set was chosen for the expansion of valence-electron wave functions at the local density approximation (LDA) level. The crystal structure was optimized by using the Broyden-Fletcher-Goldfarb-Shannon (BFGS) method. The band structure and density of states (DOS) were calculated where eigenenergy convergence of self-consistent field (SCF) was within 1.0×10^{-7} eV/atom. 340 eV was selected as energy cutoff of plane wave basis, and 4 × 4 × 2 Monkhorst-Pack grid (separation ~0.04 $Å^{-1}$) was chosen as K -point sampling in the process of calculations. Furthermore, the co-occupied Ln (La, Ce)/Sr and O/N sites were separated by reducing the space group symmetry to *P*1 (No.1). According to the ratio of co-occupied ions, each site was identified with a specific atom to avoid CASTEP calculation errors. The density of states (DOS) has alpha and beta band structures for the $Ce_{4-x}Sr_{2+x}Si_5N_{12-x}O_x$ compound. It was calculated from the Ce electron in 4f shell with spin up and spin down state.

Luminescence Properties. The luminescence properties for Pr^{3+}-doped $La_{2.31}Sr_{3.69}Si_5N_{10.31}O_{1.69}$, such as photoluminescence excitation (PLE) spectra, photoluminescence (PL) spectra, were performed on a fluorescence spectrophotometer (Hitachi F-7100, Japan). Temperature-dependent emission spectra were measured on Hitachi F-7100 equipped with TAP-02 high-temperature fluorescence attachment. The decay curves were analyzed by fluorescence spectrophotometer with a 150 W microsecond pulsed lamp as the excitation source on Edinburgh

FLS1000 fluorescence spectrophotometer. The quantum efficiency (QE) was measured by a PL quantum yield measurement system (C9920-02, Hamamatsu).

Magnetic property measurements. The powdered samples of $Ce_{2.44}Sr_{3.56}Si_5N_{10.44}O_{1.56}$ were packed into polyethylene (PE) capsules and attached to the sample holder rod on a Quantum Design PPMS system. The magnetic property of $Ce_{2.44}Sr_{3.56}Si_5N_{10.44}O_{1.56}$ under 5 - 300 K was measured at the magnetic field (30 Oe and 1000 Oe) in the zero-field-cooling (ZFC) modus and the field cooling (FC) modus, respectively.

Table of Contents

Table S1 Selected bond lengths and angles of $La_{2.31}Sr_{3.69}Si_5N_{10.31}O_{1.69}$.

Bond	Length (Å)	Bond	Length (Å)
Si1-N/O1	1.689 (7)	Si3-N6	1.775 (7)
Si1-N/O2	1.676 (7)	Si3-N7	1.747 (7)
Si1-N5	1.713 (8)	Si4-N/O3	1.716 (7)
Si1-N9	1.747 (7)	Si4-N5	1.733 (8)
Si2-N10	1.698 (7)	Si4-N6	1.733 (7)
Si2-N12	1.721 (7)	Si4-N7	1.745 (7)
Si2-N8	1.710 (8)	Si5-N11	1.731 (7)
Si2-N9	1.740 (8)	Si5-N12	1.734 (7)
Si3-N10	1.723 (7)	Si5-N/O4	1.753 (7)
Si3-N11	1.715 (7)	Si5-N8	1.742 (8)
Bond	**Angle (deg)**	**Bond**	**Angle (deg)**
Si2-N10-Si3	163.5(5)	N10-Si2-N12	107.6(4)
Si3-N11-Si5	118.8(4)	N8-Si2-N9	107.6(3)
Si2-N12-Si5	149.5(4)	N7-Si3-N6	105.9(3)
Si1-N5-Si4	144.4(5)	N6-Si3-N10	109.2(3)
Si4-N6-Si3	138.9(4)	N11-Si3-N10	114.6(4)
Si4-N7-Si3	149.5(4)	N/O3-Si4-N7	113.3(3)
Si2-N8-Si5	157.1(5)	N/O3-Si4-N5	108.6(4)
Si2-N9-Si1	167.9(5)	N5-Si4-N7	105.0(4)
N/O1-Si1-N5	117.8(4)	N11-Si5-N/O4	108.2(3)
N/O2-Si1-N5	105.7(4)	N11-Si5-N8	112.2(4)
N5-Si1-N9	105.1(4)	N12-Si5-N8	104.1(4)
N10-Si2-N9	114.1(4)	N11-Si5-N12	114.1(4)

Note:

The bond lengths of Si-N/O and Si-N in $La_{2.31}Sr_{3.69}Si_5N_{10.31}O_{1.69}$ are in the typical ranges of 1.676(7) - 1.753(7) and 1.698(7) - 1.775(7) Å, respectively, which correspond to typical values reported for other oxonitridosilicates, such as Si-N [1.704(2) - 1.780(2) Å] in $La_{3-x}Ca_{1.5x}Si_6N_{11}:Eu^{2+}$ ($x \approx 0.77$) and Si-N/O [1.61(2) - 1.82(5) Å] in $Lu_4Ba_2[Si_{12}O_2N_{16}C_3]: Eu^{2+}$.[1, 2] The bond lengths of Si-N/O are slightly shorter than that of the Si-N bonds as expected. The angle value of the (O/N) - Si - (O/N) in the tetrahedra ranging from 104.1(4) ° to 114.6(4) ° are also close to the ideal value of 109°, and the Si-N-Si angles between the Si(O/N)4 tetrahedra vary within 118.8(4) ° - 167.9(5) ° as

shown in Table S1. For $Ce_{2.44}Sr_{3.56}Si_5N_{10.44}O_{1.569}$, typically selected bond lengths and angles obtained by refined based on powder X-ray diffraction data are shown in Table S6.

Table S2 Atomic coordinates, equivalent displacement parameters, and site occupancies of $La_{2.31}Sr_{3.69}Si_5N_{10.31}O_{1.69}$.

Atom	*Wyck.*	*x*	*y*	*z*	*S.o.f.*	U_{eq}
La1/Sr1	4*e*	0.0729 (2)	0.7130 (9)	0.3399 (4)	0.50/0.50	0.0088 (1)
La2/ Sr2	4*e*	0.3323 (1)	-0.3123 (2)	0.2839 (6)	0.50/0.50	0.0047 (2)
La3/ Sr3	4*e*	0.7305 (6)	0.2702 (2)	0.5083 (8)	0.36/0.64	0.0040 (6)
La4/ Sr4	4*e*	0.8256 (7)	0.7585 (8)	0.2217 (8)	0.35/0.65	0.0068 (6)
La5/ Sr5	4*e*	0.9457 (8)	1.2455 (6)	0.0496 (8)	0.60/0.40	0.0050 (5)
Sr6	4*e*	0.4151 (4)	0.7458 (5)	0.0150 (9)	1.00	0.0030 (7)
Si1	4*e*	0.2739 (5)	0.2307 (4)	0.4003 (1)	1.00	0.0065 (4)
Si2	4*e*	0.7536 (6)	1.2625 (4)	0.1126 (1)	1.00	0.0068 (4)
Si3	4*e*	0.5418 (9)	0.7551 (4)	0.2616 (7)	1.00	0.0059 (4)
Si4	4*e*	0.4821 (1)	0.2458 (4)	0.3573 (4)	1.00	0.0071 (4)
Si5	4*e*	0.6220 (1)	0.7568 (4)	0.1036 (9)	1.00	0.0066 (4)
N1/ O1	4*e*	0.2367 (5)	-0.0331 (7)	0.3524 (4)	0.58/0.42	0.0205 (8)
N2/O2	4*e*	0.2026 (4)	0.4525 (6)	0.3601 (4)	0.58/0.42	0.0155 (7)
N3/O3	4*e*	0.5648 (5)	0.2380 (6)	0.4445 (4)	0.58/0.42	0.0151 (6)
N4/O4	4*e*	0.5826 (5)	0.7486 (6)	-0.0049 (4)	0.58/0.42	0.0154 (8)
N5	4*e*	0.3804 (5)	0.3301 (8)	0.3889 (5)	1.00	0.0151 (5)
N6	4*e*	0.4719 (5)	-0.0319 (6)	0.3049 (4)	1.00	0.0110 (5)
N7	4*e*	0.5016 (4)	0.4663 (6)	0.2837 (4)	1.00	0.0095 (6)
N8	4*e*	0.7037 (5)	0.9856 (7)	0.1237 (4)	1.00	0.0122 (7)
N9	4*e*	0.7744 (5)	1.2831 (6)	0.0091 (5)	1.00	0.0109 (7)
N10	4*e*	0.8484 (5)	1.2798 (7)	0.1861 (4)	1.00	0.0120 (8)
N11	4*e*	0.5300 (5)	0.8082 (6)	0.1553 (4)	1.00	0.0100 (6)
N12	4*e*	0.6810 (5)	1.4904 (7)	0.1340 (4)	1.00	0.0110 (5)

Table S3 Anisotropic displacement parameters (U_{iy} in Å^2) of $La_{2.31}Sr_{3.69}Si_5N_{10.31}O_{1.69}$ with standard deviations in parentheses.

Atom	U_{11}	U_{22}	U_{33}	U_{12}	U_{13}	U_{23}
La1	0.008 (6)	0.009 (5)	0.007 (8)	0.000 (7)	-0.000 (3)	-0.000 (1)
La2	0.004 (1)	0.004 (3)	0.005 (2)	0.000 (2)	-0.001 (0)	-0.000 (6)
La4	0.007 (1)	0.005 (8)	0.007 (2)	-0.000 (1)	-0.0003 (2)	-0.001 (4)
Sr1	0.008 (6)	0.009 (5)	0.007 (8)	0.000 (7)	-0.000 (3)	-0.000 (1)
Sr2	0.004 (1)	0.004 (3)	0.005 (2)	0.000 (2)	-0.001 (0)	-0.000 (6)
Sr4	0.007 (1)	0.005 (8)	0.007 (2)	-0.000 (1)	-0.000 (3)	-0.001 (4)
Sr6	0.002 (2)	0.001 (6)	0.004 (5)	0.000 (1)	-0.002 (2)	-0.000 (6)
Si1	0.006 (1)	0.006 (7)	0.006 (1)	0.001 (0)	-0.001 (2)	0.000 (2)
Si2	0.007 (4)	0.006 (1)	0.006 (4)	0.000 (0)	-0.000 (7)	-0.000 (3)
Si3	0.004 (7)	0.006 (8)	0.005 (9)	-0.001 (4)	-0.000 (6)	-0.001 (5)
Si4	0.007 (1)	0.006 (6)	0.007 (4)	-0.000 (5)	0.000 (7)	0.000 (3)
Si5	0.005 (8)	0.005 (9)	0.007 (6)	-0.000 (3)	-0.000 (2)	0.000 (7)
N1	0.025 (4)	0.017 (4)	0.018 (4)	-0.006 (3)	0.001 (3)	0.000 (3)
N2	0.013 (3)	0.014 (4)	0.019 (3)	0.008 (3)	-0.001 (3)	0.005 (3)
N3	0.011 (2)	0.017 (3)	0.015 (2)	0.000 (4)	-0.006 (1)	-0.002 (2)
N4	0.018 (4)	0.015 (4)	0.012 (3)	0.000 (3)	0.001 (3)	0.003 (3)
N5	0.011 (2)	0.017 (3)	0.015 (2)	0.000 (4)	-0.006 (1)	-0.002 (2)
N6	0.014 (2)	0.011 (2)	0.007 (2)	0.006 (1)	0.000 (4)	0.000 (8)
N7	0.012 (3)	0.010 (3)	0.007 (3)	0.005 (3)	0.000 (2)	0.003 (3)
N8	0.010 (3)	0.015 (4)	0.012 (3)	-0.001 (3)	0.002 (3)	0.002 (3)
N9	0.008 (3)	0.010 (3)	0.015 (3)	0.005 (2)	0.003 (3)	0.003 (3)
N10	0.010 (3)	0.011 (4)	0.012 (3)	0.000 (3)	-0.006 (3)	0.002 (3)
N11	0.011 (3)	0.011 (3)	0.008 (3)	0.002 (3)	0.001 (3)	0.002 (3)
N12	0.014 (2)	0.011 (2)	0.007 (2)	0.006 (1)	0.000 (4)	0.000 (8)
O1	0.025 (4)	0.017 (4)	0.018 (4)	-0.006 (3)	0.001 (3)	0.000 (3)
O2	0.013 (3)	0.014 (4)	0.019 (3)	0.008 (3)	-0.001 (3)	0.005 (3)
O3	0.011 (2)	0.017 (3)	0.015 (2)	0.000 (4)	-0.006 (1)	-0.002 (2)
O4	0.018 (4)	0.015 (4)	0.012 (3)	0.000 (3)	0.001 (3)	0.003 (3)

Table S4 Data for the Rietveld refinement of a $Ce_{2.44}Sr_{3.56}Si_5N_{10.44}O_{1.56}$ sample.

Chemical formula	$Ce_{2.44}Sr_{3.56}Si_5N_{10.44}O_{1.56}$
Formula mass (g/mol)	965.49
Crystal system	monoclinic
Space group	$P2_1/n$ (No. 14)
a (Å)	14.9028(9)
b (Å)	5.4632(8)
c (Å)	16.0085(1)
β (°)	98.995(9)
Cell volume (Å^3)	1287.36(2)
Z	4
Radiation	Cu Kα (λ = 1.54178 Å)
Diffractometer	Rigaku MiniFlex 600
Structure refinement	Topas 5
Temperature (K)	297
2ϑ range (°)	5 - 120
Step size (°)	0.01
Profile function	PV_TCHZ
R_p (%)	3.95
R_{wp} (%)	5.43
R_{exp} (%)	2.72
GoF	2.00

Table S5 Atomic positions, occupancies and temperature factors (B_{eq}) obtained in structure refinement of $Ce_{2.44}Sr_{3.56}Si_5N_{10.44}O_{1.569}$.

Atom	*Wyck.*	*x*	*y*	*z*	*S.o.f.*	B_{eq}
Ce1/Sr1	4*e*	0.0736(6)	0.7068(6)	0.3398(1)	0.48/0.52	1.23(7)/ 1.07(6)
Ce2/Sr2	4*e*	0.3324(1)	-0.3117(5)	0.2845(9)	0.60/0.40	1.23(7)/ 1.07(6)
Ce3/Sr3	4*e*	0.7289(5)	0.2735(6)	0.5073(6)	0.44/0.56	1.23(7)/ 1.07(6)
Ce4/Sr4	4*e*	0.8277(6)	0.7576(7)	0.2215(1)	0.22/0.78	1.23(7)/ 1.07(6)
Ce5/Sr5	4*e*	0.9448(7)	1.2493(7)	0.0489(6)	0.60/0.40	1.23(7)/ 1.07(6)
Ce6/Sr6	4*e*	0.4144(2)	0.7494(7)	0.0132(2)	0.10/0.90	1.23(7)/ 1.07(6)
Si1	4*e*	0.2772(5)	0.2352(1)	0.3976(5)	1.00	1.41(5)
Si2	4*e*	0.7533(5)	1.2673(1)	0.1137(5)	1.00	1.41(5)
Si3	4*e*	0.5418(9)	0.7552(5)	0.2574(5)	1.00	1.41(5)
Si4	4*e*	0.4822(5)	0.2503(1)	0.3573(4)	1.00	1.41(5)
Si5	4*e*	0.6239(6)	0.7568(4)	0.1036(9)	1.00	1.41(5)
N1/O1	4*e*	0.2416(9)	-0.0331(8)	0.3455(5)	0.61/0.39	3.13(1)/ 3.13(1)
N2/O2	4*e*	0.2073(9)	0.4525(6)	0.3601(6)	0.61//0.39	3.13(1)/ 3.13(1)
N3/O3	4*e*	0.5648(7)	0.2381(2)	0.4508(6)	0.61/0.39	3.13(1)/ 3.13(1)
N4/O4	4*e*	0.5826(5)	0.7486(6)	-0.0049(4)	0.61/0.39	3.13(1)/ 3.13(1)
N5	4*e*	0.3804(1)	0.3301(7)	0.3889(3)	1.00	0.82(1)
N6	4*e*	0.4687(8)	-0.0319(7)	0.3099(2)	1.00	0.82(1)
N7	4*e*	0.5016(4)	0.4663(6)	0.2890(7)	1.00	0.82(1)
N8	4*e*	0.7062(1)	0.9856(7)	0.1242(1)	1.00	0.82(1)
N9	4*e*	0.7744(5)	1.2815(0)	0.0097(6)	1.00	0.82(1)
N10	4*e*	0.8566(7)	1.2798(5)	0.1901(5)	1.00	0.82(1)
N11	4*e*	0.5300(5)	0.8082(5)	0.1553(4)	1.00	0.82(1)
N12	4*e*	0.6698(9)	1.4904(6)	0.1311(9)	1.00	0.82(1)

Table S6 Selected bond lengths and angles of $Ce_{2.44}Sr_{3.56}Si_5N_{10.44}O_{1.569}$.

Bond	Length (Å)	Bond	Length (Å)
Si1-N1/O1	1.730(6)	Si3-N7	1.789(9)
Si1-N2/O2	1.631(9)	Si4-N3/O3	1.784(7)
Si1-N5	1.650(8)	Si4-N6	1.713(6)
Si2-N12	1.802(1)	Si4-N7	1.672(1)
Si2-N8	1.707(9)	Si5-N11	1.755(7)
Si2-N9	1.742(1)	Si5-N12	1.639(6)
Si3-N10	1.617(8)	Si5-N4/O4	1.752(2)
Si3-N11	1.641(8)		
Bond	Angle (deg)	Bond	Angle (deg)
Si2-N10-Si3	167.1(8)	N10-Si2-N12	113.8(5)
Si3-N11-Si5	118.1(4)	N8-Si2-N9	105.9(7)
Si2-N12-Si5	146.4(8)	N6-Si3-N7	100.1(7)
Si1-N5-Si4	144.4(5)	N6-Si3-N10	106.1(7)
Si4-N6-Si3	135.8(7)	N11-Si3-N10	116.7(5)
Si4-N7-Si3	155.7(7)	N/O3-Si4-N7	114.1(8)
Si2-N8-Si5	157.1(5)	N/O3-Si4-N5	106.6(4)
Si2-N9-Si1	169.6(5)	N5-Si4-N7	105.2(7)
N1/O1-Si1-N5	116.5(5)	N11-Si5- N4/O4	106.9(4)
N2/O2-Si1-N5	106.8(5)	N11-Si5-N8	112.6(5)
N5-Si1-N9	105.5(5)	N12-Si5-N8	109.5(5)
N10-Si2-N9	112.4(6)	N11-Si5-N12	110.3(5)

Table S7 Data for the Rietveld refinement of a $La_{2.31}Sr_{3.69}Si_5N_{10.31}O_{1.69}$ sample.

Chemical formula	$La_{2.31}Sr_{3.69}Si_5N_{10.31}O_{1.69}$
Formula mass (g/mol)	956.13
Crystal system	Monoclinic
Space group	$P2_1/n$ (No. 14)
a (Å)	14.9297(5)
b (Å)	5.4799(5)
c (Å)	16.0785(4)
β (°)	98.920(9)
Cell volume (Å^3)	1299.54(2)
Z	4
Radiation	Cu Kα (λ = 1.54178 Å)
Diffractometer	Rigaku MiniFlex 600
Structure refinement	Topas 5
Temperature (K)	297
2ϑ range (°)	5 - 120
Step size (°)	0.01
Profile function	PV_TCHZ
R_p (%)	4.08
R_{wp} (%)	5.72
R_{exp} (%)	3.45
GoF	1.66

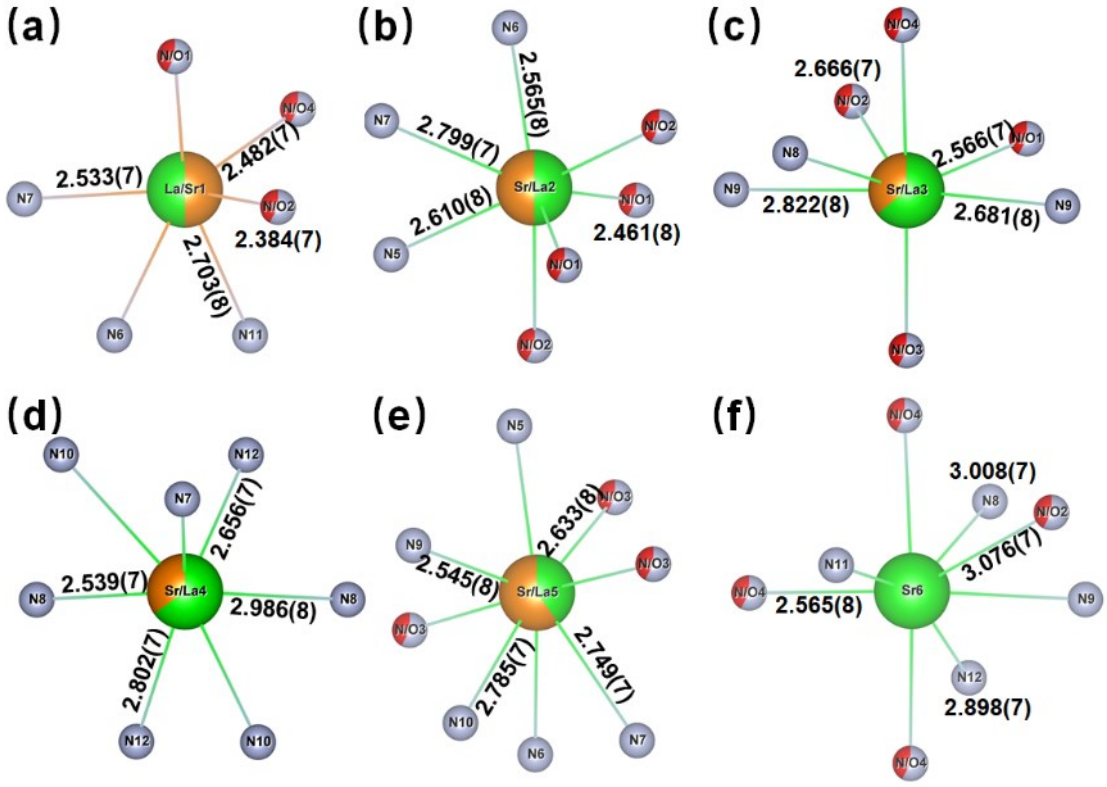

Fig. S1 Coordination spheres (a) of the heavy atom sites in $La_{2.31}Sr_{3.69}Si_5N_{10.31}O_{1.69}$ structure model with (a) La /Sr1 sites, (b) Sr / La2 sites, (c) Sr / La3 sites, (d) Sr / La4 sites, (e) Sr / La5 sites and (f) Sr6 sites.

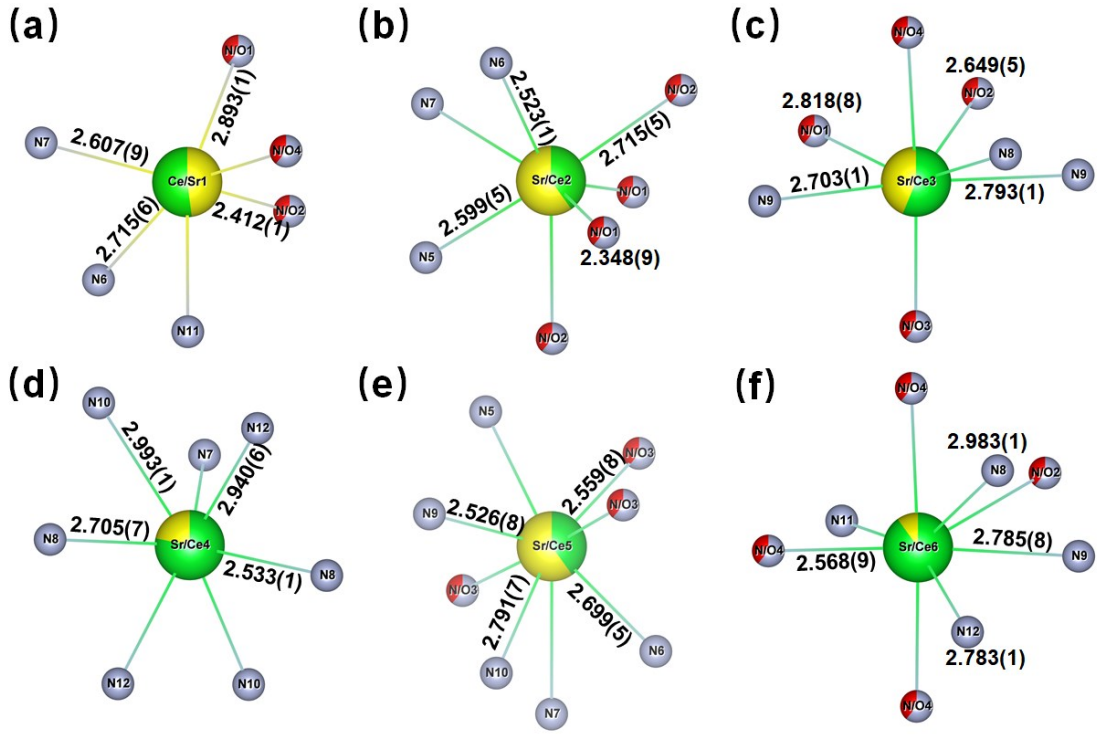

Fig. S2 Coordination spheres of the heavy atom sites in $Ce_{2.44}Sr_{3.56}Si_5N_{10.44}O_{1.56}$ with (a) Ce /Sr1 sites, (b) Sr / Ce2 sites, (c) Sr / Ce3 sites, (d) Sr / Ce4 sites, (e) Sr / Ce5 sites and (f) Sr / Ce6 sites.

Note:

The double layer of Si(O/N) tetrahedra is linked by five mixed occupied sites La/Sr (La/Sr1-La/Sr5) and a full occupied site Sr (Sr6). Coordination environments of the six atoms are illustrated in Fig. S1. The mixed occupied sites La/Sr have the coordination numbers (CN) range from six to eight. The fully occupied site Sr6 is coordinated with eight ligand atoms. The La/Sr1-ligand distances in mixed occupied sites with CN = 6 range from 2.533(7) to 2.703(8) Å (La/Sr-N), and 2.384(7) to 2.789(8) Å (La/Sr-N/O). Further La/Sr-ligand distances in mixed occupied sites La/Sr2, La/Sr3, and La/Sr4 with CN = 7 are in the ranges 2.539(7) to 2.986(8) Å (La/Sr-N) and 2.461(8) to 2.796(8) Å (La/Sr-N/O). Bond lengths of mixed occupied sites La/Sr5 and the full-occupied site Sr6 with CN = 8 are in the range of 2.545(8)-3.076(7) Å (La/Sr-N), 2.633(8)-2.785(7) Å (La/Sr-N/O), 2.632(7)-3.008(7) Å (Sr-N), 2.565 (8)-3.076(7) Å (Sr-N/O), which are in good agreement with comparable compounds.[2-5] Furthermore, the coordination of Ce/Sr for the Ce-containing compound is similar to $La_{2.31}Sr_{3.69}Si_5N_{10.31}O_{1.69}$ except the Ce/Sr6 is the mixed occupied site. And the coordination environments of six Ce/Sr mixed occupied sites are displayed in Fig. S2.

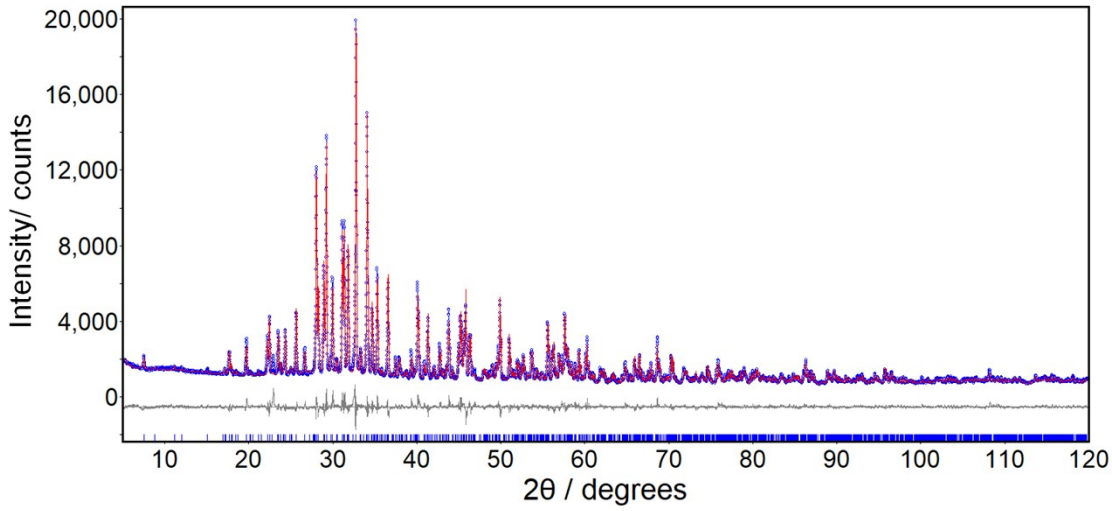

Fig. S3 Experimental data (blue dots), calculated pattern (red line) and difference profile (gray line) and the Bragg reflection positions (blue short vertical lines) for Rietveld refinements of $Ce_{2.44}Sr_{3.56}Si_5N_{10.44}O_{1.56}$.

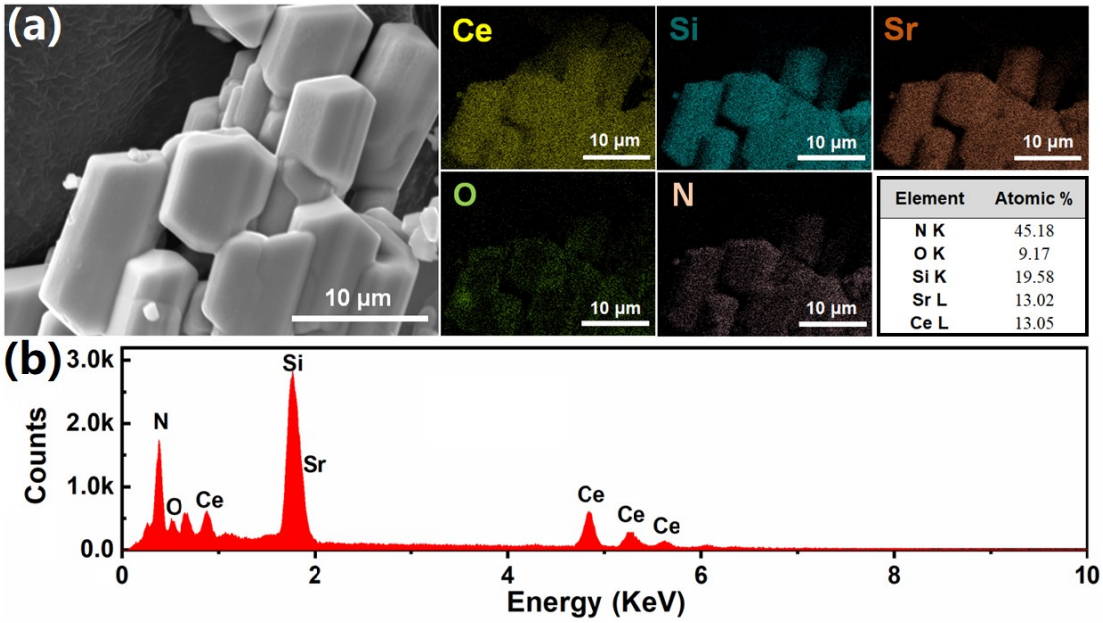

Fig. S4 Representative SEM image, elemental distributions of Ce/ Sr/ Si/ O/ N measured by EDX mapping (a) and EDS data for $Ce_{2.44}Sr_{3.56}Si_5N_{10.44}O_{1.56}$ (b).

Table S8 Results in atom% from 10 EDX point-measurements of $La_{2.31}Sr_{3.69}Si_5N_{10.31}O_{1.69}$.

Measurement	La	Sr	Si	N	O
1	13.87	13.59	21.01	43.59	7.94
2	12.20	12.55	19.20	46.21	9.84
3	14.70	13.63	19.81	43.11	8.75
4	14.55	14.25	19.66	43.39	8.16
5	11.90	13.54	17.91	48.60	8.05
6	12.06	13.66	18.74	47.39	8.15
7	12.52	13.40	18.24	46.97	8.88
8	11.77	13.28	17.68	48.82	8.45
9	15.55	14.90	21.24	41.31	7.01
10	13.18	13.40	18.95	47.30	7.17
Average	13.47	13.73	19.10	45.61	8.09

Table S9 Results in atom% from 10 EDX point-measurements of $Ce_{2.44}Sr_{3.56}Si_5N_{10.44}O_{1.56}$.

Measurement	Ce	Sr	Si	N	O
1	13.87	13.59	21.01	43.59	7.94
2	12.20	12.55	19.20	46.21	9.84
3	11.85	12.70	18.63	47.21	9.61
4	13.81	13.56	20.54	43.59	8.50
5	14.50	14.55	21.63	41.28	8.04
6	12.92	12.44	18.85	46.35	9.44
7	11.01	10.90	17.36	51.73	8.99
8	14.15	14.12	20.88	42.83	8.02
9	12.29	12.11	18.21	48.17	9.21
10	12.29	12.11	18.21	48.17	8.21
Average	12.89	12.86	19.45	45.91	8.78

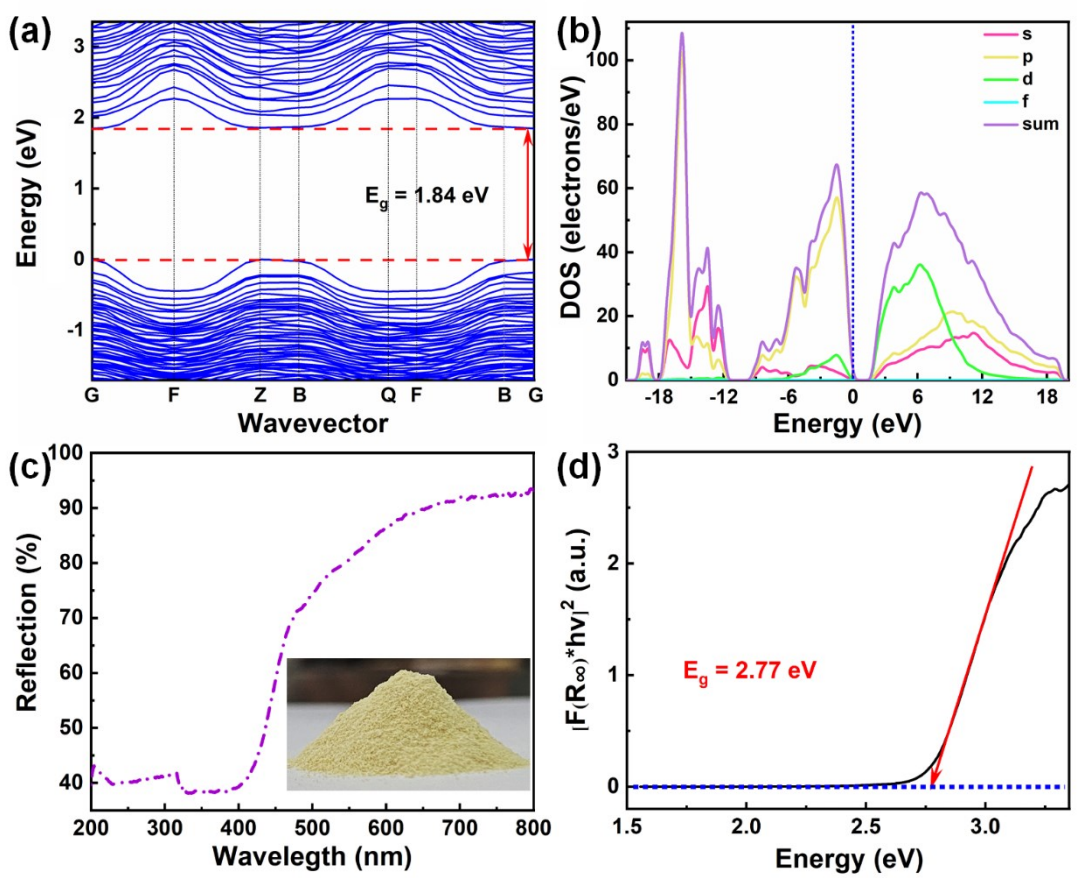

Fig. S5 Band structure (a), total and partial density of states (b) for $La_{2.31}Sr_{3.69}Si_5N_{10.31}O_{1.69}$, diffuse reflection spectra (c) of undoped $La_{2.31}Sr_{3.69}Si_5N_{10.31}O_{1.69}$ with inset of powder photo and Tauc plot (black, n = 1/2) with tangent (red) at the inflection point (d).

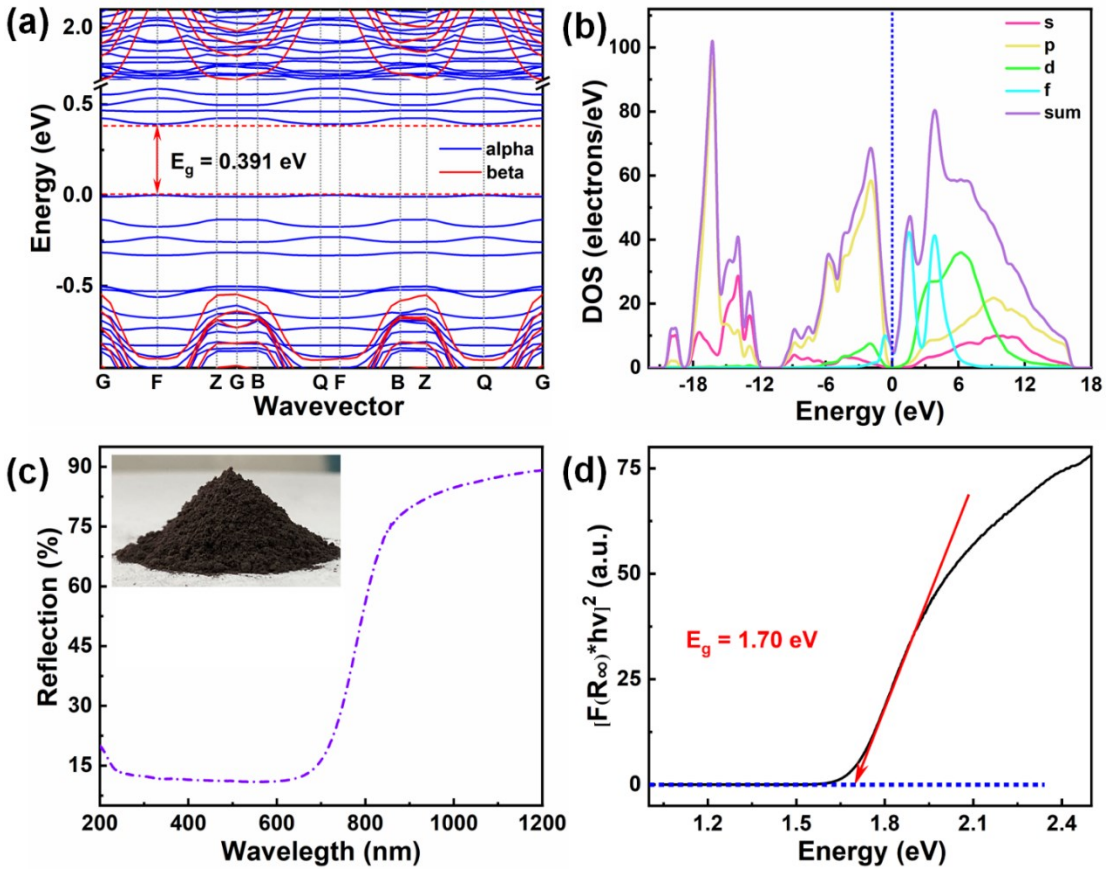

Fig. S6 Band structure (a), total and partial density of states (b) for $Ce_{2.44}Sr_{3.56}Si_5N_{10.44}O_{1.56}$, diffuse reflection spectra (c) of $Ce_{2.44}Sr_{3.56}Si_5N_{10.44}O_{1.56}$ with inset of powder photo and Tauc plot (black, n = 1/2) with tangent (red) at the inflection point (d).

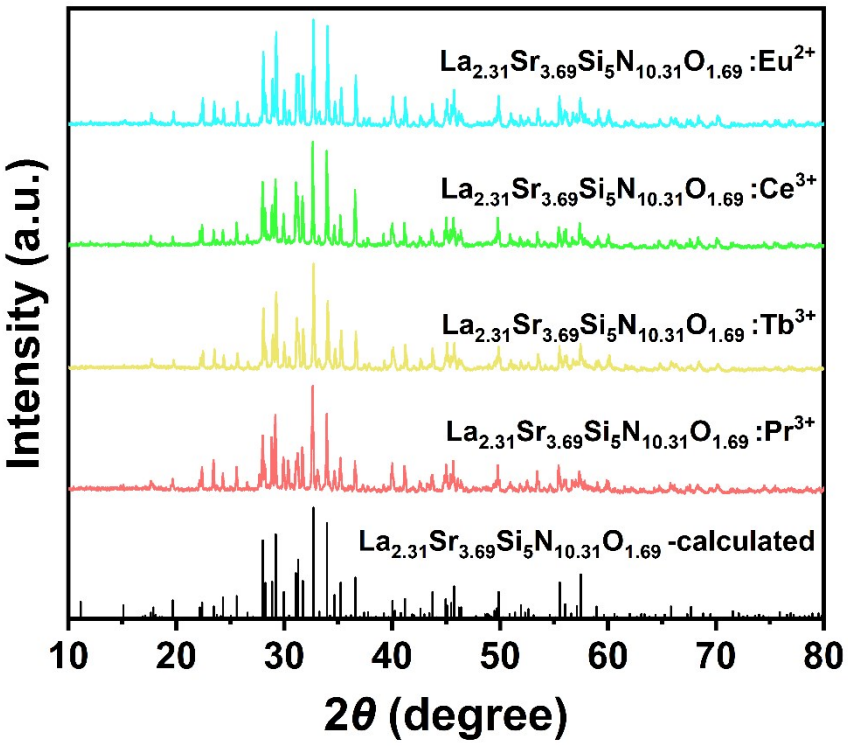

Fig. S7 The XRD patterns of Pr^{3+} -, Tb^{3+} -, Ce^{3+} -, and Eu^{2+} -doped $La_{2.31}Sr_{3.69}Si_5N_{10.31}O_{1.69}$.

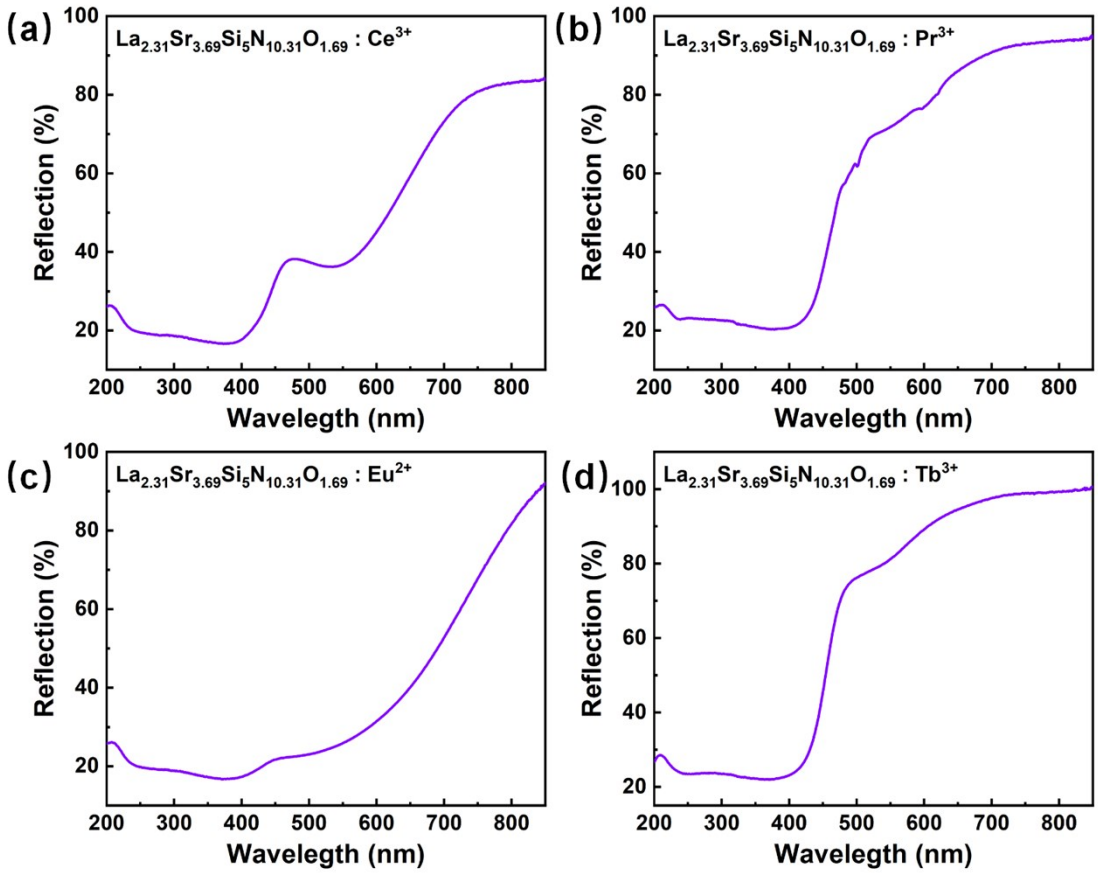

Fig. S8 The diffuse reflection spectra of phosphors for Ce^{3+}- (a), Pr^{3+}- (b) Eu^{2+}- (c) and Tb^{3+}- (d) doped $La_{2.31}Sr_{3.69}Si_5N_{10.31}O_{1.69}$.

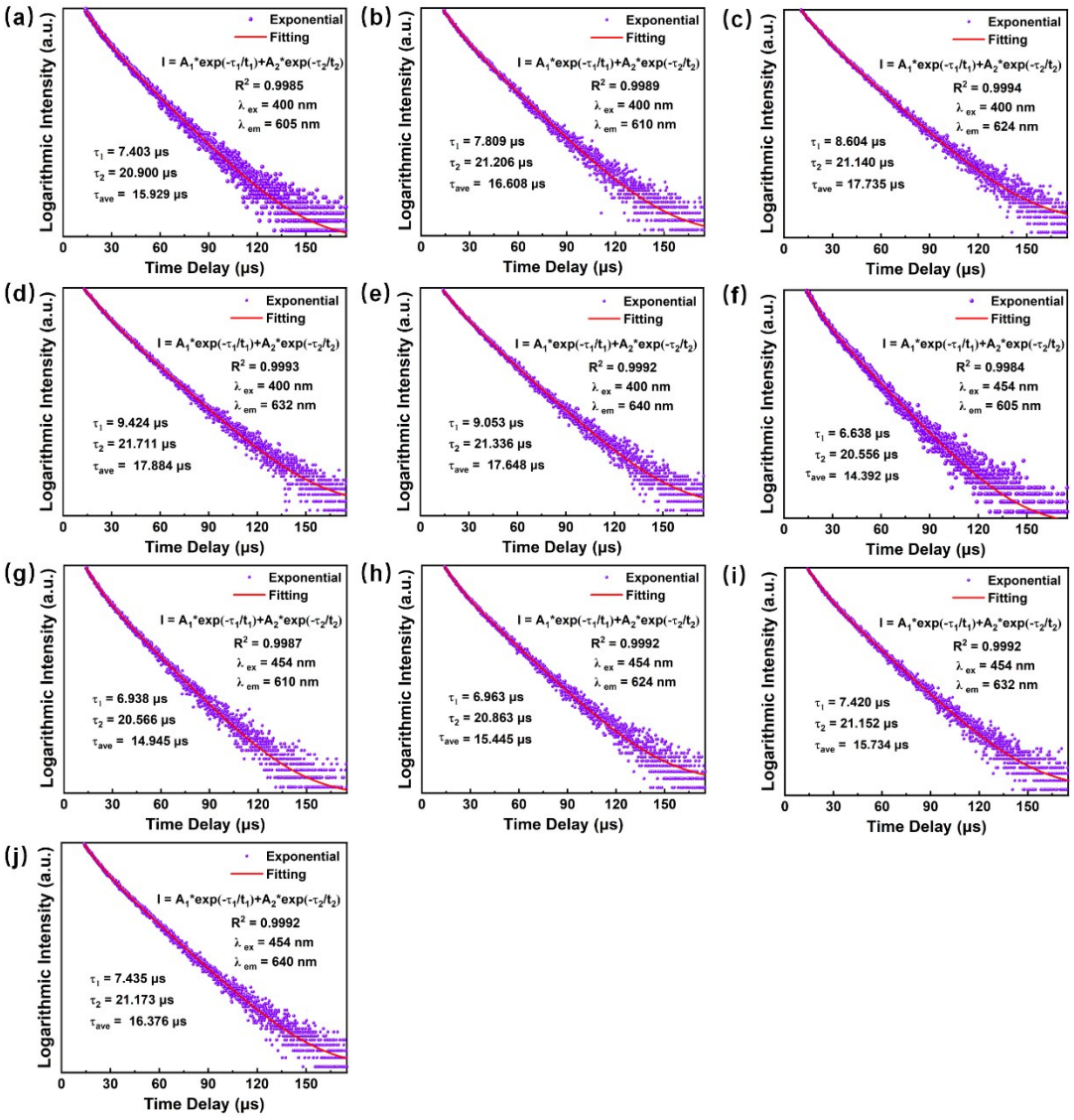

Fig. S9 Fluorescence decay curves of $La_{2.295}Sr_{3.69}Si_5N_{10.31}O_{1.69}$: $0.015Pr^{3+}$ after pulse excitation at 400 nm while monitored at 605 nm (a), 610 nm (b), 624 nm (c), 624 nm (d), and 640 nm (e); Fluorescence decay curves of $La_{2.295}Sr_{3.69}Si_5N_{10.31}O_{1.69}$: $0.015Pr^{3+}$ after pulse excitation at 454 nm while monitored at 605 nm (f), 610 nm (g), 624 nm (h), 624 nm (i), and 640 nm (j).

Table S10 Decay times and fit parameter for the measured $La_{2.295}Sr_{3.69}Si_5N_{10.31}O_{1.69}$: $0.015Pr^{3+}$.

λ_{ex} / nm	λ_{em} / nm	τ_1 / µs	τ_2 / µs	τ_{ave} / µs
400	605	7.403	21.140	15.929
400	610	7.809	21.206	16.608
400	624	8.604	21.140	17.735
400	632	9.424	21.711	17.884
400	640	9.053	21.336	17.648
454	605	6.938	20.566	14.945
454	610	6.638	20.556	14.392
454	624	6.963	20.863	15.445
454	632	7.420	21.152	15.734
454	640	7.435	21.173	16.376

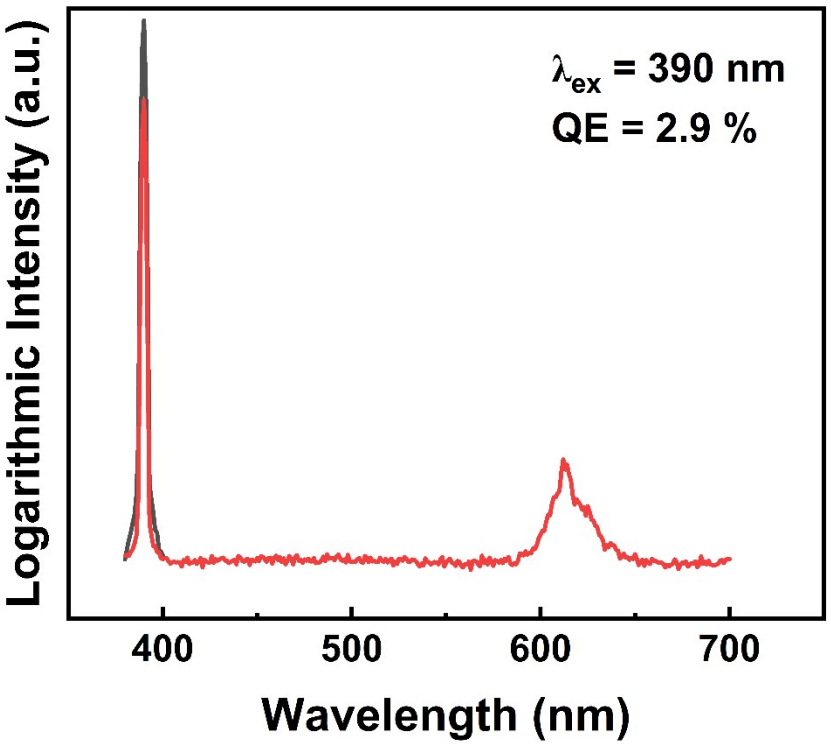

Fig. S10 The quantum efficiency (QE) of phosphor for $La_{2.295}Sr_{3.69}Si_5N_{10.31}O_{1.69}$: $0.015Pr^{3+}$.

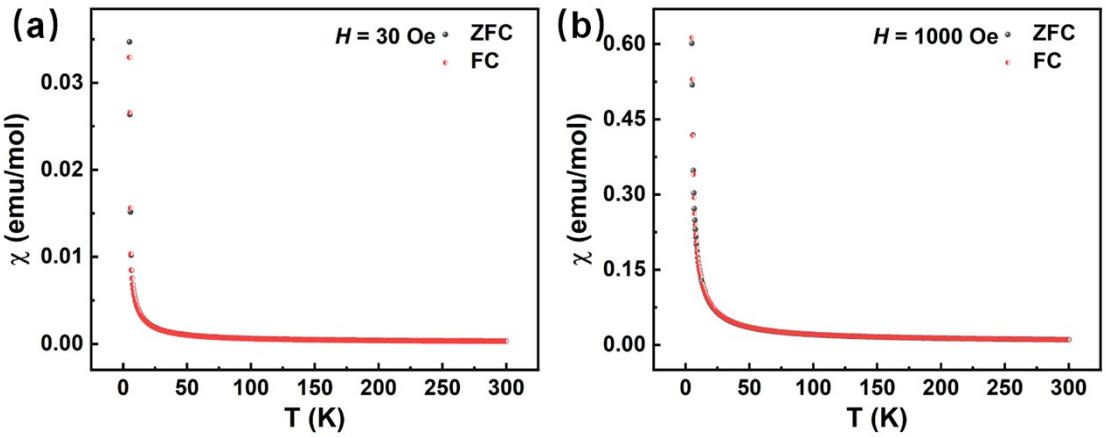

Fig. S11 Measurements conducted in zero-field-cooled/ field-cooled mode (ZFC/FC) with an applied field of 30 Oe (a) and 1000 Oe (b).

Note:

The $Ce_{2.44}Sr_{3.56}Si_5N_{10.44}O_{1.56}$ powder shows a black color which is not suitable for the phosphor host. The temperature dependence of the inverse magnetic susceptibility of $Ce_{2.44}Sr_{3.56}Si_5N_{10.44}O_{1.56}$ measured at the magnetic flux density of 30 Oe and 1000 Oe are shown in Fig. S11. The measurements conducted in zero-field-cooled/field-cooled (ZFC/FC) at different external fields. There is no ferromagnetic ordering observed in $Ce_{2.44}Sr_{3.56}Si_5N_{10.44}O_{1.56}$ below the temperature T ≈ 5 K so that this compound is probably paramagnetic.

Reference

1. C. Maak, L. Eisenburger, J. P. Wright, M. Nentwig, P. J. Schmidt, O. Oeckler and W. Schnick, *Inorg. Chem.*, 2018, **57**, 13840-13846.
2. C. Maak, D. Durach, C. Martiny, P. J. Schmidt and W. Schnick, *Chem. Mater.*, 2018, **30**, 3552-3558.
3. C. Maak, R. Niklaus, O. Oeckler and W. Schnick, *Z. Anorg. Allg. Chem.*, 2019, **645**, 182-187.
4. L. Neudert, D. Durach, F. Fahrnbauer, G. B. M. Vaughan, W. Schnick and O. Oeckler, *Inorg. Chem.*, 2017, **56**, 13070-13077.
5. X. M. Wang, C. H. Wang, X. J. Kuang, R. Q. Zou, Y. X. Wang and X. P. Jing, *Inorg. Chem.*, 2012, **51**, 3540-3547.